

Mapping Disorder in Entropically Ordered Crystals

James Antonaglia,¹ Greg van Anders,¹ and Sharon C. Glotzer^{1,2,3,4}

¹*Department of Physics, University of Michigan, Ann Arbor, MI 48109, USA*

²*Department of Chemical Engineering, University of Michigan, Ann Arbor, MI 48109, USA*

³*Department of Materials Science and Engineering, University of Michigan, Ann Arbor, MI 48109, USA*

⁴*Biointerfaces Institute, University of Michigan, Ann Arbor MI 48109, USA*

(Dated: March 19, 2018)

Systems of hard shapes crystallize due to entropy. How is entropy distributed among translational and rotational microscopic contributions? We answer this question by decomposing thermal fluctuation of crystals of hard hexagons into collective modes, a generalization and quantification of the Onsager picture of hard rod liquid crystals. We show that at densities both near densest packing and near the solid-hexatic melting transition, solids of hard regular hexagons hold most of their entropy in translational degrees of freedom.

Plato’s order/chaos dichotomy [1] has a long intellectual history that achieves its most precise mathematical formulation in the theory of phase transitions [2]. However, phase transitions can be driven by entropy [3–5], which is historically associated with disorder [6]. Entropy-driven phase transitions confront Plato’s dichotomy with an apparent paradox: a macroscopically ordered system can exhibit more microscopic disorder than a macroscopically disordered system [7, 8]. Entropy-driven liquid crystalline [7] and crystalline order [9] can be rationalized through intuitive arguments for simple enough model systems, but resolving the paradox for more complex types of order [10–13] requires a detailed description of the entropy in an ordered system. Quantifying entropy contributions is complicated by the fact that entropy arises from statistical considerations, and is inherently macroscopic unlike energy, which trivially decomposes into a sum of microscopic contributions.

Here, we quantify contributions to the entropy of hard particle crystals by decomposing thermal fluctuations in two-dimensional systems of hard regular polygons into collective modes. Collective vibrational (phonon) modes have been studied previously for hard spheres [14, 15], and propagating rotational (libron) modes have been studied in detail in molecular crystals [16–18]. We compute the dispersion relations for phonon and libron modes for hard hexagons [19], and show that the macroscopic system entropy is partitioned into phonon and libron contributions. From these contributions, we construct a “map,” by wavevector, of the contributions of microscopic order that lead to macroscopic order. For macroscopic order in systems at densities just above crystallization and close to maximal packing, we find a predominance of translational disorder. We find that the reason for the predominance of translational order, however, is different at low and high densities. Moreover, we find that between density extremes systems receive primary contributions from both translational and orientational disorder at different wavevectors. Our results give a concrete picture of “disorder within order,” and offer an intuitive explanation of recent, counterintuitive findings on the behavior of densely packed anisotropic colloids.[20]

Dispersion relations relate the frequency and wavelength of vibrational and librational modes in crystals. We computed dispersion relations for phonons and librons in a crystal of

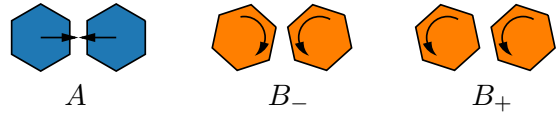


FIG. 1. Microscopic degrees of freedom which contribute to collective modes. Below each image is listed the parameter names used for the second derivatives of $\mathcal{U}_{1,2}$, the effective interparticle potential, with respect to that mode. The first and second relative displacements correspond to stiffnesses that penalize gradients in both crystal displacements and body orientation, respectively. The third type of displacement corresponds to a stiffness that penalizes homogeneous or cooperative rotation and gives rise to a libron dispersion gap. There is no corresponding cooperative translation term because of global translational symmetry.

hard hexagons from NVT simulation using the hard-particle Monte Carlo (HPMC) plugin [21] for HOOMD-blue [22, 23]. We use systems of $N = 10,000$ hexagons near the hexatic-solid transition [19], and 2,500 hexagons for higher densities. In addition, we validated our analytical and numerical approaches with systems of hard disks. In all cases, we initialized systems into hexagonal lattices, thermalized and equilibrated at a selected density, and sampled over 1×10^7 Monte Carlo (MC) sweeps at high density, and 5×10^7 MC sweeps at low density. Four independent samples were run at each density. From these MC data we computed dynamical matrix elements at all wavevectors \vec{k} commensurate with the periodic boundary conditions using ensemble averages of statistically independent samples.

To calculate dynamical matrix elements, we constructed a linear elastic model (see SI for details) of the system that assumes that anisotropic hard core interactions can be modeled via effective, entropic pair interactions [9], $\mathcal{U}_{1,2}(|\vec{r}_1 - \vec{r}_2|, \theta_1, \theta_2)$, which yield the parameters

$$\frac{\partial^2 \mathcal{U}_{1,2}}{\partial r_{1,2}^2} = A, \quad \frac{\partial^2 \mathcal{U}_{1,2}}{\partial (\theta_1 + \theta_2)^2} = B_+, \quad \frac{\partial^2 \mathcal{U}_{1,2}}{\partial (\theta_1 - \theta_2)^2} = B_-, \quad (1)$$

where \vec{r}_i and θ_i describe particle positions and orientations. A and B_{\pm} determine the eigenvalues of the dynamical matrix (see Fig. 1 for illustration and SI for mathematical form) and

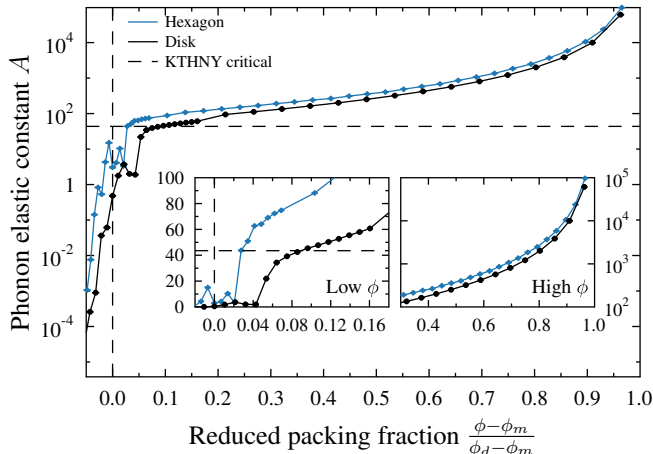


FIG. 2. Phonon elastic constant for crystals of hard disks (black) and hexagons (blue) at all densities, scaled to range from 0 (melting) to 1 (densest packing). The black dashed line indicates the critical value for A at the hexatic-solid transition, predicted by the KTHNY melting theory. Both solids exhibit similar stiffness constants at the same normalized densities at high density. Insets are magnifications in the vicinity of the melting transition and densest packing, respectively. Error bars indicating $1\text{-}\sigma$ standard deviations of elastic constants from best fits of four independent simulations to theoretical dispersion curves are smaller than the plot markers.

thus function as effective, entropic stiffness parameters [24]. We extracted them from dispersion relations computed with MC data using least squares fitting.

At high densities, when dislocations are absent, we use displacement covariance analysis (DCA) [25] to compute dispersion relations. DCA uses equipartition to relate small, thermal deviations x_i to a dynamical matrix K_{ij} according to $\langle x_i x_j \rangle = k_B T K_{ij}^{-1}$, where the x_i of interest are phonon modes $u_\mu(\vec{k})$,

$$u_\mu(\vec{k}) = \frac{1}{\sqrt{N}} \sum_{\alpha} (r_{\mu}^{\alpha} - \langle r_{\mu}^{\alpha} \rangle) e^{-i\vec{k} \cdot \langle \vec{r}^{\alpha} \rangle}, \quad (2)$$

and libron modes $\theta(\vec{k})$,

$$\theta(\vec{k}) = \frac{1}{\sqrt{N}} \sum_{\alpha} \left[(\theta^{\alpha} - \langle \theta^{\alpha} \rangle) \bmod \frac{2\pi}{6} \right] e^{-i\vec{k} \cdot \langle \vec{r}^{\alpha} \rangle}. \quad (3)$$

Here, r_{μ}^{α} is the μ spatial component of the position of the center of particle α , θ^{α} is the orientation of the body of the particle with respect to the positive x -axis, and N is the total number of particles. Particles' rotation symmetry is removed by the modulo $2\pi/6$ operation. We fix units by taking the particle circumdiameter and the thermal energy $k_B T$ to be unity. At lower densities, where dislocations become important and particles are able to diffuse from their lattice positions, we adapt a method that decomposes density fluctuations into contributions from transverse and longitudinal hydrodynamic wave modes [26]. This method is tolerant of dislocations and does not assume particles vibrate closely around

well-defined lattice positions, but is more computationally intensive than simple DCA. See SI for details.

We determined the density-dependent, effective elastic constants for both phonon and libron modes in hard hexagon crystals. We validated our results for A by extracting the melting transition density, at which the Kosterlitz-Thouless-Halperin-Nelson-Young (KTHNY) theory [27] predicts $2A/\sqrt{3}$ should change discontinuously from the universal value of 16π to 0, and find good agreement with melting densities reported in [19] (see Fig. 2). Results for hard disks are also shown for comparison. For both hexagons and disks Fig. 2 data are given at densities ϕ expressed with respect to dense packing density ϕ_d (hexagons: 1, disks: $\pi/(2\sqrt{3})$) and melting density ϕ_m (hexagons: 0.710, disks: 0.719 [19]) in the form $(\phi - \phi_m)/(\phi_d - \phi_m)$. The near collapse of the data observed for the phonon elastic constant between hexagons and disks reveals the interesting result that using ordinary, translational sound, it is difficult at moderate densities and above to distinguish the difference between hexagon- and disk-shaped particles if density is scaled appropriately.

We present in Fig. 3 phonon and libron dispersion relations for a range of densities for high symmetry points in the Brillouin zone. These frequencies are computed from eigenvalues of the dynamical matrix multiplied by the inverse mass matrix, which has diagonal elements $1/m$ for phonon modes and $1/I = 48/(5m)$ in reduced units for libron modes. We find several features of the dispersion relations that are common at all densities. First, we find deviations between our simulation data and the linear elastic model are only appreciable near the edge of the Brillouin zone. The edges correspond to short distances, and is precisely where we would expect a linear elastic model of hard interactions to break down. Although deviations increase with density as expected, we find that the linear elastic model provides a good approximation for most of the Brillouin zone, even for relatively high densities of 0.9. Second, we find that phonon modes are always ungapped, which is guaranteed by Goldstone's theorem. Third, we find that the libron modes are gapped at all densities, but that their group velocity increases rapidly with system density.

What do these features imply the contributions are to the macroscopic entropy of the system? It can be shown (see SI) that the fluctuation spectrum yields a mode-by-mode decomposition of the configurational entropy (up to overall additive constants) according to

$$S = -\frac{1}{2} \sum_{i, \vec{k}} \ln(\omega_i^2(\vec{k})). \quad (4)$$

Here, $\omega_i(\vec{k})$ are the dispersion frequencies, and the sum extends over all mode types i corresponding to longitudinal and transverse phonon modes and libron modes at all wavevectors \vec{k} in the first Brillouin zone. Brillouin zones are shown in Fig. 3, as "entropy maps," in which all points are colored according to the mode that provides the dominant contribution to the system entropy at that wavevector, using Eq. 4.

This analysis produces a similar entropy map at densities just above the hexatic-solid transition (0.722) and close to dense packing (0.9) in which entropy at all wavevectors comes

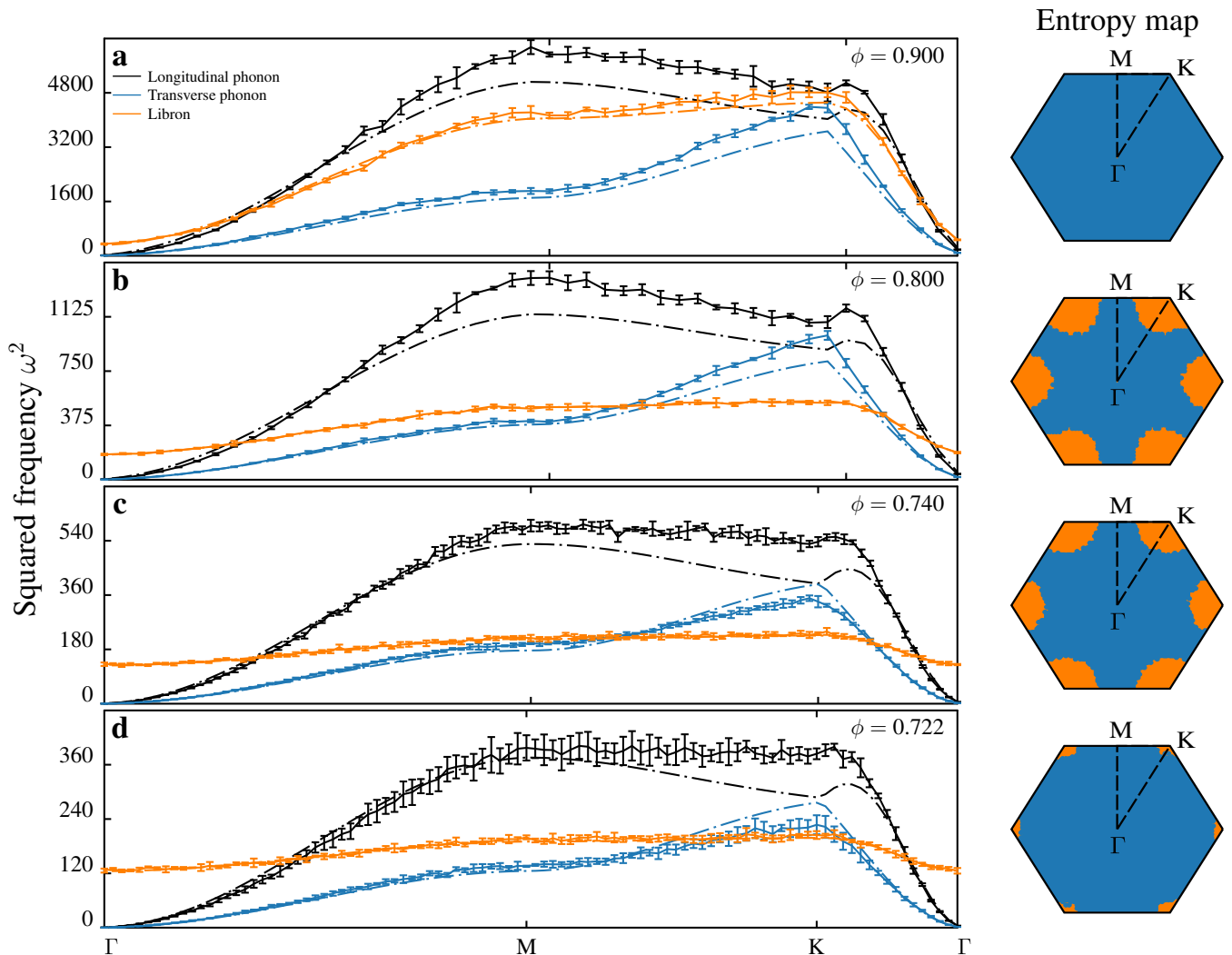


FIG. 3. Dispersion relation for hard hexagon crystals at various packing fractions. All dispersion relations decrease with decreasing density, but the phonon dispersions become ill-defined at densities close to the hexatic-solid phase transition. Right panels are the first Brillouin zone colored corresponding to the lowest frequency mode at each \vec{k} -vector; orange indicates the libron mode and blue indicates the transverse phonon mode. Broken lines indicate theoretical dispersion relations with best-fit stiffness parameters. Error bars are 1- σ sample standard deviations of the dispersion frequencies averaged from four independent simulations.

predominantly from translational disorder. The predominance of translational disorder just above the hexatic-solid transition arises because although the libron group velocity is small, the gap in the libron spectrum is sufficiently large to put the libron dispersion above the phonon dispersion throughout the Brillouin zone (save for wavevectors at the very edge of the Brillouin zone where we expect the harmonic approximation to breakdown). This is in contrast to what occurs at high densities. At high densities the phonon group velocity itself has increased by an order of magnitude (cf. vertical scales in Fig. 3a vs. d). In addition, we find there is an increase in the libron gap, but that this increase is much less dramatic than the increase in the libron group velocity, which becomes similar in scale to the phonon group velocity.

Our observation of ungapped phonon modes is a conse-

quence of Goldstone's theorem, but our observation of a gapped libron spectrum is the result of more subtle field-theoretic effects. For systems of isotropic particles, it has been shown that although crystals break both translational and rotational symmetry, the absence of Goldstone modes associated with rotational symmetry breaking is due to linear relations among translation and rotation generators that render the Goldstone modes associated with rotational symmetry breaking redundant [28]. For systems of anisotropic particles, rotation generators contain additional terms that correspond to particle body rotations which introduce additional degrees of freedom. These degrees of freedom can be shown (see SI) to always couple to the global rotation generator as a mass term in a linear elastic model. The existence of coupling between the generator of global rotations and the generator of

body rotations implies that, in generic situations, the libron modes for anisotropic colloids or molecules should be gapped, whereas Goldstone’s theorem requires that phonon modes remain ungapped [29]. Thus, librational gaps should appear in any crystal or hexatic phase of anisotropic particles with global orientational order. Because of this, we expect that systems of anisotropic particles that melt from crystals with quasi-long range translational and long range orientational order into hexatic or other phases with quasi-long range orientational order but without translational order will exhibit entropy maps similar to those found here. We note that, practically, the identification of the signatures of solid-hexatic transition found here were far less computationally intensive to produce than approaches that were used to confirm the transition elsewhere [19]. In contrast, if a system were to “melt” from a crystal with well-defined orientational order to a plastic crystal, we would expect a dramatically different entropy map.

At high densities, the predominance of translational disorder at all wavevectors arose through a combination of the gap in the libron spectrum and the comparable group velocity for phonon and libron modes. In our model systems we found that translational disorder predominated at all wavevectors at all densities at or above 0.9. Because the libron gap is a consequence of global orientational order, and because dense packing of highly anisotropic shapes generically leads to strong constraints on both particle positions and orientations, we would expect that similar computations in other systems would lead to similar phonon and libron group velocities. We therefore expect the predominance of translational disorder to be a generic feature of densely packed colloids. If this is so, it would help to explain recently reported, unexpected results from inverse-design [30] indicating that non-space-filling shapes are thermodynamically preferred in model sys-

tems of hard colloids even at densities above 0.99.[20] In the context of the present results, this finding can be rationalized because systems stand to gain more entropy through rotational modes – which the entropy map shows are restricted at all wavevectors at high densities – than through translational modes. This is most easily achieved by slight rounding of the particles into non-space-filling shapes, as observed in Ref. [20].

We decomposed the total entropy of an entropically stabilized solid into microscopic contributions from collective modes of particle motion. We showed for a simple hard hexagon solid that translational and rotational degrees of freedom contribute different amounts of entropy at different wavevectors, extending the Onsager picture of hard rod liquid crystals [3, 7, 31] to hard particle crystals. Our method is applicable to any entropically stabilized solid in which the particles exhibit harmonic motion about equilibrium positions, and it is generalizable to three dimensions.

ACKNOWLEDGMENTS

We thank X. Mao and R. Kamien for helpful discussions. This work was supported by the National Science Foundation Graduate Research Fellowship Grant No. DGE 1256260 to J.A., and a Simons Foundation Investigator Award to S.C.G. Any opinions, findings, and conclusions or recommendations expressed in this material are those of the authors and do not necessarily reflect the views of the National Science Foundation. Data analysis in this work was performed partially using Freud, an open-source Python-driven analysis toolkit [32]. The computational workflow and data management were primarily supported by the signac data management framework [33].

-
- [1] R. D. Archer-Hind *et al.*, *The Timaeus of Plato* (Macmillan, 1888)
 - [2] L. D. Landau, *Zh. Eksp. Teor. Fiz.* **11**, 19 (1937)
 - [3] L. Onsager, *Ann. New York Acad. Sci.* **51**, 627 (1949)
 - [4] B. Alder and T. Wainwright, *J. Chem. Phys.* **27**, 1208 (1957)
 - [5] W. W. Wood and J. D. Jacobson, *J. Chem. Phys.* **27**, 1207 (1957)
 - [6] R. Clausius, *Abhandlungen Über Die Mechanische Wärmetheorie* (Friedrich Vieweg und Sohn, Braunschweig, 1864)
 - [7] D. Frenkel, *Physica A: Statistical Mechanics and its Applications* **263**, 26 (1999)
 - [8] D. Frenkel, *Nat. Mater.* **14**, 9 (2015)
 - [9] G. van Anders, D. Klotsa, N. K. Ahmed, M. Engel, and S. C. Glotzer, *Proc. Natl. Acad. Sci. U.S.A.* **111**, E4812 (2014)
 - [10] A. Haji-Akbari, M. Engel, A. S. Keys, X. Zheng, R. G. Petschek, P. Palffy-Muhoray, and S. C. Glotzer, *Nature* **462**, 773 (2009)
 - [11] P. F. Damasceno, M. Engel, and S. C. Glotzer, *Science* **337**, 453 (2012)
 - [12] U. Agarwal and F. A. Escobedo, *Nat. Mater.* **10**, 230 (2011)
 - [13] J. Henzie, M. Grünwald, A. Widmer-Cooper, P. L. Geissler, and P. Yang, *Nat. Mater.* **11**, 131 (2012)
 - [14] F. H. Stillinger, *J. Chem. Phys.* **46**, 3962 (1967)
 - [15] K. Honda, *Prog. Theor. Phys.* **55**, 1024 (1976)
 - [16] V. Schomaker and K. N. Trueblood, *Acta Cryst. B* **24**, 63 (1968)
 - [17] G. Venkataraman and V. C. Sahni, *Rev. Mod. Phys.* **42**, 409 (1970)
 - [18] J. C. Raich, *J. Chem. Phys.* **55**, 3901 (1971)
 - [19] J. A. Anderson, J. Antonaglia, J. A. Millan, M. Engel, and S. C. Glotzer, *Phys. Rev. X* **7**, 021001 (2017)
 - [20] R. Cersonsky, G. van Anders, P. M. Dodd, and S. C. Glotzer, *Proc. Natl. Acad. Sci. USA* **In Press** (2018), 10.1073/pnas.1720139115
 - [21] J. A. Anderson, M. E. Irrgang, and S. C. Glotzer, *Comp. Phys. Commun.* **204**, 21 (2016)
 - [22] J. Anderson, C. Lorenz, and A. Travesset, *J. Comp. Phys.* **227**, 5342 (2008)
 - [23] J. Glaser, T. D. Nguyen, J. A. Anderson, P. Lui, F. Spiga, J. A. Millan, D. C. Morse, and S. C. Glotzer, *Comp. Phys. Commun.* **192**, 97 (2015)
 - [24] M. A. Bates and D. Frenkel, *J. Chem. Phys.* **112**, 10034 (2000)
 - [25] B. Hess, *Phys. Rev. E* **62**, 8438 (2000)
 - [26] C. Walz and M. Fuchs, *Phys. Rev. B* **81**, 134110 (2010)
 - [27] D. Nelson and B. Halperin, *Phys. Rev. B* **19** (1979)

- [28] H. Watanabe and H. Murayama, Phys. Rev. Lett. **110**, 2401 (2013)
- [29] T. Brauner and H. Watanabe, Phys. Rev. D **89**, 085004 (2014)
- [30] G. van Anders, D. Klotsa, A. S. Karas, P. M. Dodd, and S. C. Glotzer, ACS Nano **9**, 9542 (2015)
- [31] D. Frenkel, J. Phys. Chem. **91**, 4912 (1987)
- [32] E. S. Harper, M. Spellings, J. Anderson, and S. C. Glotzer, "freud," (2016)
- [33] C. S. Adorf, P. M. Dodd, and S. C. Glotzer, (2016), arXiv:1611.03543